Proton-Proton Triple Scattering at 430 MeV*

P. LIMON, L. PONDROM, S. OLSEN, AND P. KLOEPPEL†
University of Wisconsin, Madison, Wisconsin

AND

R. HANDLER‡ AND S. C. WRIGHT
University of Chicago, Chicago, Illinois

(Received 27 December 1967)

The Wolfenstein parameters D, R, A, R', and A', and the polarization P have been measured at 430 MeV and 65° in the c.m. system, and D, R, A, and $R'+A'$ have been measured at 115° in the c.m. system. The equations relating these observables to the complex amplitudes of the p-p spin matrix have been solved for the amplitudes. The results agree well with amplitudes calculated from a phase-shift analysis which includes p-p scattering data at several energies and angles.

I. INTRODUCTION

THE measurements reported here represent a further extension of earlier work applying spark chambers to the study of polarization phenomena in nucleon-nucleon scattering.[1] The basic experimental configuration is the same as Ref. 1, with the exception that an automatic wire spark chamber system connected to an on-line computer was used.[2] This system handled event rates up to 20/sec and gave much greater statistical accuracy than was previously obtained with film. With this equipment the triple-scattering parameters A, R, A', R', and D, and the polarization P have been measured at 430 MeV and 65° in the c.m. system to an absolute error of about ± 0.015, and at 115° in the c.m. system to an absolute error of about ± 0.04. The geometrical configurations used in these measurements and described in this paper may seem unusual, especially at 65°, because the four Wolfenstein parameters were not measured separately in four experiments, but rather four independent linear combinations of the parameters were measured. The reason for this was that the first two linear combinations, where the highest statistical accuracy was obtained, were used in a T-invariance test which has been previously reported.[3]

The experimental configurations, geometrical and electronic alignment techniques, on-line computer programs, and systematic error studies are described below. This description applies equally well to the T-invariance test of Ref. 3. A direct solution to the amplitudes appearing in the p-p scattering matrix at 430 MeV and 65° is also obtained and compared with the results calculated from a phase-shift analysis fit. An effort is made to present a complete description of the experiment, which makes some repetition of earlier published work unavoidable. A general familiarity with p-p triple scattering and spark-chamber techniques has been assumed, however. The proceedings of a very recent conference on nucleon-nucleon scattering furnishes complementary experimental and theoretical information.[4]

II. EXPERIMENTAL PROCEDURE

A. General

For p-p scattering in the laboratory frame, define $\mathbf{k}_i$ and $\mathbf{k}_f$ as the initial and final proton momenta, respectively, and $\hat{n}_i=(\mathbf{k}_i\times\mathbf{k}_f)/|\mathbf{k}_i\times\mathbf{k}_f|$ as the normal to the scattering plane. The initial beam polarization is referred to in terms of the unit vectors $(\hat{k}_i,\hat{s}_i,\hat{n}_i)$, where $\hat{s}_i=\hat{n}_i\times\hat{k}_i$, and the final polarization of the scattered proton is referred to the unit vectors $(\hat{k}_f,\hat{s}_f,\hat{n}_f)$, where $\hat{n}_f=\hat{n}_i$ and $\hat{s}_f=\hat{n}_f\times\hat{k}_f$. If parity is conserved, the final spin vector $\langle\boldsymbol{\sigma}\rangle$ is given by

$$\langle\boldsymbol{\sigma}\rangle I_P(\theta,\phi)=I_0(\theta)[(P+D\langle\boldsymbol{\sigma}_i\cdot\hat{n}_i\rangle)\hat{n}_f+(A\langle\boldsymbol{\sigma}_i\cdot\hat{k}_i\rangle+R\langle\boldsymbol{\sigma}_i\cdot\hat{s}_i\rangle)\hat{s}_f+(A'\langle\boldsymbol{\sigma}_i\cdot\hat{k}_i\rangle+R'\langle\boldsymbol{\sigma}_i\cdot\hat{s}_i\rangle)\hat{k}_f], \quad (1)$$

where $I_0(\theta)$ is the unpolarized differential cross section, $I_P(\theta,\phi)=I_0(\theta)(1+P\langle\boldsymbol{\sigma}_i\cdot\hat{n}_i\rangle)$, and the parameters P, D, A, R, A', and R' are functions of the energy and polar angle θ. The terms in Eq. (1) proportional to $\langle\boldsymbol{\sigma}_i\rangle$ change sign when the initial spin is reversed, an effect which was used in the design of the experiment.

Two experimental configurations, A and B, are shown in Fig. 1. The incident polarized beam was produced by scattering through 13.5° from a beryllium target inside the cyclotron, yielding an initial polarization $P_1=0.535\pm 0.025$,[5] oriented normal to the plane of the figure. The solenoid S had 1.49×10^6 A turns, sufficient to rotate the proton magnetic moment through 90°. The solenoid field could be reversed to orient the spin

* Supported in part by the U. S. Atomic Energy Commission under Contract No. AT(11-1)-881, COO-881-148 and in part by the National Science Foundation.

† Present address: Monmouth College, Monmouth, Ill.

‡ Present address: University of Wisconsin, Madison, Wis.

[1] R. Roth, E. Engels, S. C. Wright, P. Kloeppel, R. Handler, and L. Pondrom, Phys. Rev. **140**, 1533 (1965). This paper contains references to earlier work.

[2] J. Barney, P. Kloeppel, P. Limon, L. Pondrom, R. Handler, and S. C. Wright, Nucl. Instr. Methods **54**, 66 (1967).

[3] R. Handler, S. C. Wright, L. Pondrom, P. Limon, S. Olsen, and P. Kloeppel, Phys. Rev. Letters **19**, 933 (1967).

[4] Rev. Mod. Phys. **39**, 495 ff. (1967).

[5] N. E. Booth (private communication).

either to the left, as shown in Fig. 1, or to the right. All of the triple-scattering measurements were made with the bending magnet B_1 in the incident beam, which used the anomalous g factor of the proton to precess the magnetic moment to a final angle of 45° with respect to the momentum. Thus for geometry A, or left p-p scattering, with the solenoid energized, $\langle\boldsymbol{\sigma}_i\cdot\hat{n}_i\rangle=0$, $\langle\boldsymbol{\sigma}_i\cdot\hat{k}_i\rangle=\pm P_1/\sqrt{2}$, and $\langle\boldsymbol{\sigma}_i\cdot\hat{s}_i\rangle=\pm P_1/\sqrt{2}$. The plus sign applies to left solenoid rotation and the minus sign applies to right solenoid rotation. With the solenoid off, $\langle\boldsymbol{\sigma}_i\cdot\hat{k}_i\rangle=\langle\boldsymbol{\sigma}_i\cdot\hat{s}_i\rangle=0$ and $\langle\boldsymbol{\sigma}_i\cdot\hat{n}_i\rangle=P_1$. For geometry B, or right p-p scattering, the signs of $\hat{n}_i$ and $\hat{s}_i$ are reversed. Protons with this polarization were then scattered through $\theta_{\rm lab}=30°$ (65° in the c.m. system), using target protons in liquid hydrogen. The target contained 0.9 g/cm² of liquid hydrogen. The scattered solid angle accepted was roughly 1 msr at the target. (The exact solid angle depended on radial focusing in the second bending magnet B_2 described below.) Equation (1) shows that for left p-p scattering the final spin with solenoid energized was of the form

$$\langle\boldsymbol{\sigma}\rangle=[P\hat{n}_f\pm(P_1/\sqrt{2})(A+R)\hat{s}_f\pm(P_1/\sqrt{2})(A'+R')\hat{k}_f], \tag{2}$$

where the plus and minus signs again refer to solenoid orientation. The final spin with the solenoid off was of the form

$$\langle\boldsymbol{\sigma}_f\rangle=\frac{P+DP_1}{1+P(\mathbf{P}_1\cdot\hat{n})}. \tag{3}$$

Equation (2) illustrates one unusual feature of these triple-scattering measurements. A mixture of A and R appears in the final transverse polarization in the scattering plane, and a mixture of A' and R' appears in the final longitudinal polarization. The bending magnet B_2 represents the other unusual feature. The final transverse and longitudinal spins were not measured separately. In configuration A the bending magnet B_2 precessed the spin component at 75° into 90° so that this component could be analyzed by scattering a third time from a carbon analyzer. In configuration B the spin component at 15° was measured. We define the asymmetry distributions observed in the carbon analyzer as $N(\Phi)=1+\epsilon\cos\Phi+\delta\sin\Phi$. The angle Φ is defined such that $\Phi=0$ corresponds to a third scatter to the left, in the plane of Fig. 1, and $\Phi=\frac{1}{2}\pi$ corresponds to an up scatter. Thus ϵ is referred to as the left-right asymmetry, and δ as the up-down asymmetry. The detailed operation of the carbon analyzer will be described below. It is sufficient here to characterize the analyzer by some average analyzing power P_3 which is a function of the proton energy E (305 MeV at 30° in the lab) and the polar angle region of accepted carbon scatters. Then for solenoid plus (left spin rotation), Eq. (2) yields observed up-down asymmetries

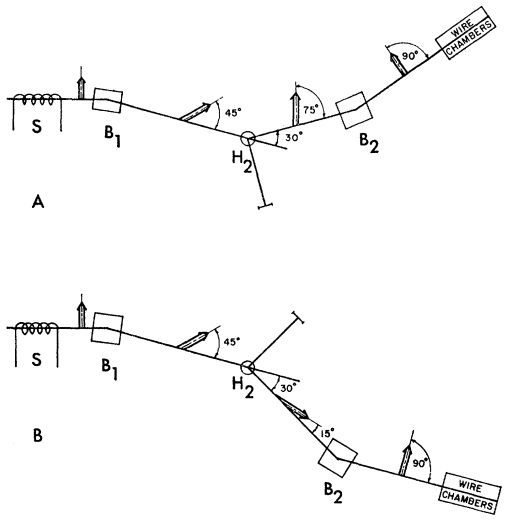

FIG. 1. Geometries A and B. Double arrows represent spin directions. The solenoid S is assumed to be excited for left spin rotation. The purpose of the bending magnets is described in the text.

$$\begin{aligned}
\delta_A&=-\frac{(P_1P_3)}{\sqrt{2}}[(A+R)\cos15°+(A'+R')\sin15°],\\
\delta_B&=-\frac{(P_1P_3)}{\sqrt{2}}[(R-A)\cos75°+(A'-R')\sin75°],\\
\delta_C&=-\frac{(P_1P_3)}{\sqrt{2}}[(R-A)\sin75°-(A'-R')\cos75°],\\
\delta_D&=-\frac{(P_1P_3)}{\sqrt{2}}[(A+R)\sin15°-(A'+R')\cos15°].
\end{aligned} \tag{4}$$

Reversing the sign of the solenoid current reversed all of the above asymmetries. The terms δ_C and δ_D refer to the geometries shown in Fig. 2, which were chosen to measure final spin directions perpendicular to the directions shown in Fig. 1. The corresponding left-right asymmetries with solenoid on also follow from Eq. (2):

$$\begin{aligned}
&\text{Geom. } A \text{ and } D\text{:}\quad \epsilon_P=PP_3,\\
&\text{Geom. } B \text{ and } C\text{:}\quad \epsilon_P=-PP_3.
\end{aligned} \tag{5}$$

These asymmetries did not depend on the solenoid field orientation, but on $\langle\boldsymbol{\sigma}_i\cdot\hat{n}_i\rangle=0$. With the solenoid off, the up-down asymmetries should all be zero, and the left-right asymmetries follow from Eq. (3):

$$\begin{aligned}
&\text{Geom. } A \text{ and } D\text{:}\quad \epsilon_D=(P+DP_1)/(1+PP_1),\\
&\text{Geom. } B \text{ and } C\text{:}\quad \epsilon_D=-(P-DP_1)/(1-PP_1).
\end{aligned} \tag{6}$$

The possibility of nonzero up-down asymmetries, indicating a violation of parity, will be discussed below.

A schematic view of the carbon polarimeter and the

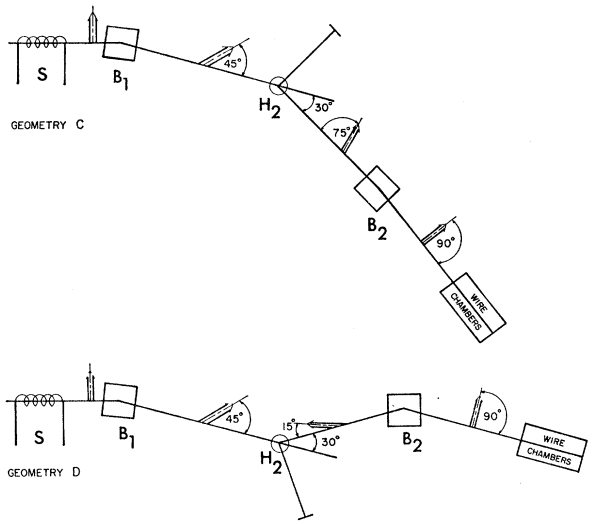

FIG. 2. Geometries *C* and *D*. The final spin components measured here are orthogonal to the ones measured in *A* and *B*. These four diagrams complete the 30° lab or 65° c.m. measurements.

trigger scintillation counters, without the second bending magnet B_2, is shown in Fig. 3. Three spark chambers before the 13 g/cm² carbon block were used to define the incident direction, and three spark chambers after the carbon block were used to define the scattered direction. Scintillator sizes were as follows: defining counter No. 1, $3\times4\times\frac{1}{8}$ in.; transmission counter No. 2, $12\times12\times\frac{1}{4}$ in.; anticoincidence counter No. $\bar{3}$, 12-in.-diam circle $\frac{1}{4}$ in. thick; counter No. 4, $2\times2\times\frac{1}{4}$ in. used for alignment tests; and recoil counter No. 5, $6\times6\times\frac{3}{8}$ in. A *p-p* scatter in the hydrogen target with both the scattered proton and its recoil being detected, followed by a *p*-C scatter in the carbon block through a polar angle greater than ~5° (defined by $\bar{3}$), triggered the spark chambers. The detection of both protons completely eliminated the small contribution from inelastic events at this energy. In geometry *B* with 10^8 protons/sec incident on the hydrogen target the typical trigger rate was 15 events/sec. Each spark chamber was composed of a single gap formed by a high-voltage conducting plane and a ground plane. Each plane was made of 0.004-in. Al wires spaced 24 wires/in. The two planes were oriented with wires running at 90° to each other, defining *X* and *Y* coordinates. The *Z* coordinate was defined by the axis of the system. Magnetostrictive delay-line techniques were used to obtain two coordinates from each chamber for each event.[6] To be acceptable, an event could have only one spark in each chamber. The computer program described below and in Ref. 2 was used to reconstruct each event. The spark-chamber system with the carbon block removed was a powerful instrument for determining positions and slopes of the proton beams defined by the various configurations, and was used extensively in the geometrical-alignment procedures described below.[7]

B. Alignment

The critical phases of the geometrical alignment procedure, which applied to all geometries, were incident-beam energy and direction, scattered-beam direction, and spin-precession angles in magnets B_1 and B_2. The spark-chamber system with the carbon removed was used to determine in a short time the beam center to a few millimeters and the beam slope relative

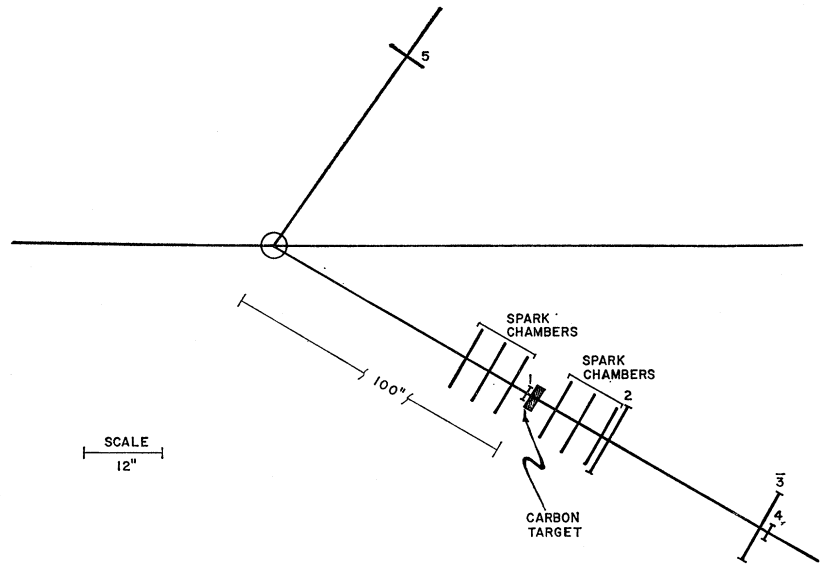

FIG. 3. Schematic diagram of the trigger counter and spark-chamber configuration, without the second bending magnet B_2 inserted. The distance between the hydrogen target and counter No. 1 has been foreshortened, but the drawing is otherwise to scale.

[6] For a more complete description of the basic electronic system see Ref. 2.
[7] The alignment programs are described in more detail in P. Limon, Ph.D. thesis, University of Wisconsin (unpublished).

to the spark chamber axis to a milliradian. The relative orientation of the spark-chamber axis in space was determined with a transit fixed to the cart which held the chambers, and a mirror mounted on the wall.

The beam geometry had to be invariant under excitation of the solenoid or a systematic bias might have been introduced. This invariance was obtained by moving the solenoid until the beam did not shift when the polarity was reversed. In order to calculate the proper bending angles for spin preparation, a careful measurement of the beam momentum was made. This was done by bending the beam in a symmetric window-frame magnet, and measuring the bending angle with the polarimeter. The central field of the magnet was measured with a NMR probe and the fringing field was mapped with a Hall-effect probe. The result of the momentum measurement was $p=995\pm9$ MeV/c, with a corresponding kinetic energy $T=429\pm7$ MeV. The error was derived from estimated uncertainties in the bending angle and the field map.

Once the beam energy was known, the bending angle for magnet B_1 was calculated, and found to be 17.25° for a 45° rotation of the spin relative to the momentum. This angle was surveyed by rotating the spark-chamber cart from the direct beam line to a line at 17.25°. B_1 was then properly set on the intersection of these two lines and its excitation was varied until the center of the beam traveled down the center of the spark-chamber system. This established the initial polarization vector $\mathbf{P}_1$ at an angle of 45.0°±0.4° relative to the momentum. The hydrogen target position was then chosen along this beam line, and the scattering angle (30° or 54.68°) was surveyed using a transit. The intersection of the line thus defined with the final scattered proton beam line after the second spin-precession magnet determined the location of that magnet, B_2. The final scattered proton beam line was set by rotating the spark-chamber system through the appropriate net space angle (bending angle plus precession angle) relative to the incident-beam direction. The hydrogen target and the recoil counter at the proper conjugate angle were then installed. The excitation of B_2 was adjusted until protons scattered through the correct angle as determined by the recoil counter were also bent through the correct angle as determined by the axis of the spark-chamber system.

The spark coordinates were measured relative to fiducial wires in each plane. These wires were mechanically aligned at the beginning of the experiment in such a way that they were mutually perpendicular in each chamber, and that the points formed by their intersections were all along a line parallel to the Z axis and perpendicular to the chamber planes. A special calibration check routine was performed several times a day to ensure proper operation of this coordinate system. First the velocities of propagation of the sound waves in the magnetostrictive lines were measured by shorting each chamber through a second fiducial wire which was at a known distance from the first fiducial. The computer stored 500 such numbers from each plane, and calculated average velocity constants for each magnetostrictive line. These constants varied the order of 1%. The carbon block was then removed from the spark-chamber system, and unscattered proton tracks were recorded. The resulting coordinates were fitted to straight lines. The difference between the fitted track and the actual output coordinate was calculated for each plane, and this difference was averaged over a large number of tracks. The result of this average δ_j could be several standard deviations for the jth plane, and was interpreted as a correction to the zero point. An infinite set of valid zero-point corrections could be defined, however, by the transformation $\delta'_j=\delta_j+\alpha+\beta Z_j$, where Z_j is the position of the jth plane along the axis of the system, and α and β are arbitrary constants. This arbitrariness was eliminated by choosing α and β such that the geometric centers of counters No. 1 and No. 4 coincided with the Z axis of the coordinate system. Thus the computer and the proton beam were used to find the edges and centers of the scintillation counters, and the line joining these centers was used to fix the zero-point corrections δ_j. The new velocity constants and zero-point corrections were then stored in the computer and used to reconstruct scattered tracks.

C. Data Collection

Four weeks were spent collecting data in the four geometries of Figs. 1 and 2. The geometries were measured in sequence, since each one required about one day to set up. The computer received events at a typical rate of 15/sec, and fitted each one to two straight lines intersecting in the carbon scatterer. If the event passed certain selection criteria, its polar and azimuthal scattering angles from the carbon block were stored in the computer in a matrix which divided the polar angles between 5° and 20° into 10 equal bins, and the azimuthal angles between 0° and 360° into 20 equal bins. The computer selected events in an effort to eliminate systematic bias. The rejected events, about 70% of all triggers, fell into the following categories: (a) 3% had one or more zeros in the scalers, due to misfirings of the chambers; (b) 25% had more than two magnetostrictive line pulses due to multiple sparks or edge sparks; (c) 8% had excessive kinks in the track or a poor fit to two straight lines, that is, the particle scattered somewhere other than in the carbon; (d) 22% had an incoming angle greater than 2° relative to the axis of the polarimeter; (e) 10% appeared to strike the anticoincidence counter, but triggered the system due to an anticounter inefficiency or a scatter after the spark-chamber system; (f) 25% were eliminated because the outgoing proton trajectory when rotated through 360° about the incoming proton trajectory (the cone test) was not completely within an 8-in.-diam circle centered in the last spark chamber; and (g) 7%

appeared to strike the anticoincidence counter if the cone test was applied. Category (d) was due to the large geometrical acceptance from finite target and counter sizes. The criterion of category (f) made the last chamber smaller than it actually was (10×10 in.) to eliminate edge effects. The criterion of category (g) was applied to eliminate events which, if scattered through the same polar angle but a different azimuthal angle, would not be counted. The computer averaged the $\theta_C-\Phi$ matrix over θ_C from 5° to 20° and performed a least-squares fit to the Φ distribution $N(\Phi)=1+\epsilon\cos\Phi+\delta\sin\Phi$ every 2000 accepted events. These results, as well as the total matrix and the number of rejected events in each category, were printed about every 20 min.

According to Eqs. (2) and (4), the true up-down asymmetries should reverse with the polarity of the solenoid. To eliminate systematic up-down bias, the solenoid was reversed once or twice a day. Data were also taken in each geometry with the solenoid off, to measure D [Eq. (6)]. Table I shows the raw data obtained from the computer for each of the four geometries at 65°. Note that the up-down asymmetry was zero within statistical error with the solenoid off, and changed sign within statistical error when the solenoid was reversed, giving no evidence of an up-down bias. The left-right bias was more difficult to treat. Equation (5) indicates that the left-right asymmetry observed with the solenoid on should have reversed as the apparatus was moved from the left side of the incident beam (geometries A and D) to the right side of the beam (geometries B and C). Equation (6), on the other hand, has no particular symmetry. Thus the left-right bias could be studied, but not with the frequent cycling back and forth that was possible with the solenoid. Apparently geometries A and D gave systematically larger values of ϵ than did B and C, with a bias $\frac{1}{2}(\epsilon_A+\epsilon_B)=0.01$. A number of symmetry tests involving the trigger counters, wire chambers, and magnetostrictive lines were made, but the true source of this bias was never found.

TABLE I. Asymmetries of the form $N(\Phi)=1+\epsilon\cos\Phi+\delta\sin\Phi$ observed in the geometries of Figs. 1 and 2. N is the total number of accepted events in each case. The solenoidal magnetic field was along the proton direction of motion, giving left rotation, when the setting was plus. The signs of ϵ and δ are chosen such that spin-up, which scatters to the left from carbon, gives a positive ϵ. The expected value of χ^2 was 18: 20 data in Φ and 2 parameters.

Geom.	Solenoid	ϵ	δ	N	χ^2
A	−	0.1584	0.1615	234 025	12.6
A	+	0.1634	−0.1616	261 520	14.1
A	off	0.3007	0.0141	48 000	21.1
B	−	−0.1453	0.1658	212 033	12.7
B	+	−0.1387	−0.1561	200 046	15.9
B	off	0.0616	−0.0071	38 011	17.4
C	−	−0.1285	0.0004	50 000	16.4
C	+	−0.1466	−0.0049	50 000	11.8
C	off	0.0521	0.0073	94 000	13.9
D	−	0.1707	0.0880	128 000	16.7
D	+	0.1656	−0.0559	146 000	14.2
D	off	0.3152	0.0226	22 000	9.3

The product P_1P_3 of the incident-beam polarization times the average analyzing power of the spark chamber system for 300-MeV protons enters into the δ relations in Eq. (4). To determine the triple-scattering parameters A, R, A', and R', only this product need be determined. This measurement was performed in the direct proton beam, degraded from 430 to 300 MeV by Al absorbers. The results are listed in Table II. Here the asymmetry δ should have vanished with the solenoid off, and ϵ should have vanished with the solenoid excited. Also, $|\delta|$ with the solenoid on should have equaled $|\epsilon|$ with the solenoid off. All of these criteria are well satisfied by the data of Table II, giving no evidence of any systematic biases in the direct beam. The "corrected" value of P_1P_3 listed is slightly greater than the combined observed asymmetry. This effect is due to the fact that different polar angles were accepted in geometries $ABCD$ than in the direct beam, leading to a different average analyzing power. The very small values of ϵ in the first two rows of Table II indicated that the solenoid was rotating the proton spin through 90°±0.7°.

TABLE II. 300-MeV calibration. These data were taken with the spark-chamber polarimeter in the direct proton beam. The bending magnet B_1 was not excited. The resulting "corrected" $P_1P_3=0.3112\pm0.0059$.

Solenoid	ϵ	δ	N	χ^2
−	−0.0048	0.3132	40 000	17.2
+	0.0010	−0.2943	40 000	18.3
off	0.3194	−0.0069	40 000	6.8
combined	0.3091		120 000	

Figure 4 illustrates the geometries E, F, and G which were used to study the conjugate proton angle: 115° in the c.m., or 54.68° in the laboratory. Geometries E and F measured $A-R$ and $A+R$ at 115° c.m. system, and G measured $R'+A'$. These configurations were chosen because the setup was a straightforward task after the completion of the 65° studies. The final two weeks of the run were devoted to these measurements. The scattered proton energy at this laboratory angle was only 115 MeV. The short range of these protons required that the carbon block be only 2.2 g/cm² thick. This change decreased the scattering efficiency, so that a larger fraction of protons struck the anticoincidence counter than before. The finite anticoincidence efficiency resulted in a factor of 2 higher event rejection ratio. The sensitivity of the analyzer to proton polarization at this lower energy was also decreased. This sensitivity could be determined by exploiting the fact that the p-p polarization is odd about 90° in the c.m. system. Thus the left-right asymmetries observed with the solenoid on could be used to calibrate the analyzer:

$$P_1P_3'(115°)=P_1P_3(65°)\times\epsilon_p(115°)/\epsilon_p(65°), \quad (7)$$

where ϵ_p refers to the corrected left-right asymmetries with the solenoid on. The computer programs handled the events in the same way as previously described. The observed up-down asymmetries had a simpler form than at 65° because the bending magnet B_2 was only used in one case, and then for a 90° precession (G). Thus for left spin rotation in the solenoid, one has

$$\delta_E=-\frac{(P_1P_3')}{\sqrt{2}}(R-A),$$
$$\delta_F=-\frac{(P_1P_3')}{\sqrt{2}}(R+A), \quad (8)$$
$$\delta_G=+\frac{(P_1P_3')}{\sqrt{2}}(R'+A').$$

Here R, A, R', and A' are the parameters at 55° in the laboratory or 115° in the c.m. system. They are independent of the quantities defined in Eq. (4). Reversing the solenoid reversed all signs. The equations for solenoid off are similar to Eq. (6).

TABLE III. Raw data from the asymmetries observed in the three geometries in which the proton scattered at 115° c.m.

Geom.	Solenoid	ϵ	δ	N	χ^2
E	−	0.0755	0.0542	59 000	19.1
E	+	0.0653	−0.0425	60 000	16.8
E	off	0.1315	0.0098	50 000	19.8
F	−	−0.0541	0.0498	50 000	10.4
F	+	−0.0501	−0.0363	50 000	18.7
F	off	−0.0038	0.0169	14 000	23.6
G	−	−0.0615	0.0149	60 000	7.4
G	+	−0.0619	−0.0084	60 000	12.7
G	off	0.0124	0.0037	60 000	28.6

Table III gives the raw asymmetries observed in the three geometries at 115° in the c.m. system. The statistical accuracy was poorer than at 65°, and the analyzing power was lower, leading to very small asymmetries. Within the statistical error, however, the asymmetries exhibit the same characteristics as in Table I. The up-down bias was still absent, and the left-right bias was still present, favoring left, but with less statistical conviction.

III. RESULTS AND ANALYSIS

The two up-down asymmetries for solenoid "plus" and solenoid "minus" for each geometry of Tables I and III were combined by averaging $\delta=\frac{1}{2}(\delta_+-\delta_-)$ to give the data of Table IV. The left-right asymmetries ϵ_p were averaged on the two sides of the beam: $\epsilon_P=\frac{1}{2}[\epsilon_P(L)-\epsilon_P(R)]$ to eliminate the left bias. This operation was performed separately for the 65° and 115° data. The solenoid-off asymmetries ϵ_D were corrected for the left bias by multiplying the right scattering ϵ_D's by $1+\frac{1}{2}\times[\epsilon_P(L)+\epsilon_P(R)]$ and dividing the left scattering ϵ_D's

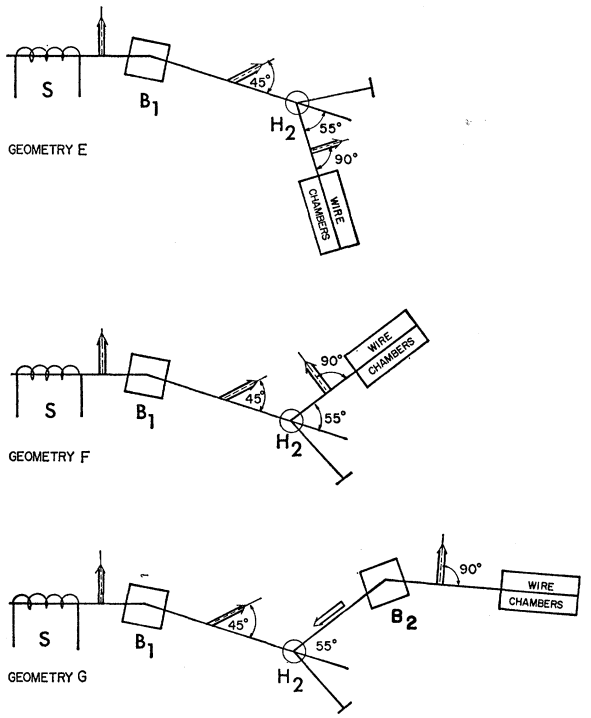

FIG. 4. Geometries E, F, and G at 54.68° in the lab, or the conjugate angle 115° in the c.m. system. Geometries E and F measured only final transverse spin components, giving $A-R$ and $A+R$, respectively. For G, the magnet B_2 precessed the final spin through 90° relative to the momentum, thus measuring $A'+R'$.

by the same factor. These various operations yielded the corrected asymmetries listed in Table IV.

From these corrected asymmetries the triple-scattering parameters could be calculated by inverting Eqs. (4) and (8), and using the calibrations $P_1P_3=0.311\pm0.006$ and $P_1P_3'=0.131\pm0.006$. These operations yielded the parameters A, R, A', and R' at 65° and A, R, and $(A'+R')$ at 115°. To obtain A' and R' separately at 115°, T invariance was assumed, which

TABLE IV. Corrected asymmetries for the various geometrical configurations.

Geom.	$\theta_{c.m.}$	δ	Std. dev.
	Up-down asymmetries		
A	65°	−0.1616	±0.0020
B	65°	−0.1610	±0.0020
C	65°	−0.0028	±0.0064
D	65°	−0.0720	±0.0027
E	115°	−0.0484	±0.0041
F	115°	−0.0431	±0.0064
G	115°	−0.0116	±0.0058
	Left-right asymmetries		
	$\theta_{c.m.}$		Std dev
ϵ_P	65°	0.1522	±0.0013
ϵ_P	115°	0.0643	±0.0025
ϵ_D	65° left	0.2941	±0.0055
ϵ_D	65° right	0.0436	±0.0041
ϵ_D	115° left	0.0037	±0.0070
ϵ_D	115° right	0.1256	±0.0066

TABLE V. Final results for P, D, R, A, R', and A'.

	Std. dev.
$\theta_{c.m.}=65°$	
$A=$ 0.296	±0.013
$R=$ 0.498	±0.015
$A'=$ 0.289	±0.016
$R'=-0.415$	±0.017
$P=$ 0.262	±0.013
$D=$ 0.599	±0.015
$\theta_{c.m.}=115°$	
$A=-0.028$	±0.033
$R=$ 0.492	±0.039
$A'=$ 0.217	±0.031
$R'=-0.360$	±0.055
$D=$ 0.557	±0.043

relates the four parameters: $\tan 54.68°=(A+R')/(A'-R)$. This assumption is consistent with the results of Ref. 3. All of these final data are listed in Table V. In order to obtain P and D from the corrected left-right asymmetries of Table IV, the beam polarization $P_1=0.535\pm0.025$ had to be used in conjunction with Eqs. (5) and (6). The values of D obtained from the left and right sides of the beam were statistically consistent and were averaged to give the final results in Table V.

If invariance under parity and time reversal, and identity of the two nucleons are assumed, the nucleon-nucleon scattering matrix can be written in terms of five complex amplitudes:

$$M(\theta,\phi)=a+c(\boldsymbol{\sigma}^{(1)}\cdot\hat{n}+\boldsymbol{\sigma}^{(2)}\cdot\hat{n})+m(\boldsymbol{\sigma}^{(1)}\cdot\hat{n}\boldsymbol{\sigma}^{(2)}\cdot\hat{n}) +(g+h)\boldsymbol{\sigma}^{(1)}\cdot\hat{P}\boldsymbol{\sigma}^{(2)}\cdot\hat{P}+(g-h)\boldsymbol{\sigma}^{(1)}\cdot\hat{K}\boldsymbol{\sigma}^{(2)}\cdot\hat{K}. \quad (9)$$

This matrix is written in the p-p c.m. system. If $\mathbf{k}$ and $\mathbf{k}'$ are, respectively, the initial and final relative momentum vectors in this frame, then $\hat{n}=\mathbf{k}\times\mathbf{k}'/|\mathbf{k}\times\mathbf{k}'|=\hat{n}_i=\hat{n}_f$. The other unit vectors are defined as $\hat{K}=(\mathbf{k}'-\mathbf{k})/|\mathbf{k}'-\mathbf{k}|$, and $\hat{P}=(\mathbf{k}'+\mathbf{k})/|\mathbf{k}'+\mathbf{k}|$. In the nonrelativistic limit $\hat{P}=\hat{k}_f$ and $\hat{K}=\hat{s}_f$ defined earlier. The five complex amplitudes a, c, m, g, and h are functions of the energy E and the scattering angle $\bar{\theta}$. Thus apart from an over-all phase (determined by Coulomb interference), nine independent experiments at a given angle and energy would in principle allow a direct solution of these amplitudes independent of a phase-shift analysis. The interest in such a direct solution has been pointed out by Schumacher and Bethe.[8] The calculation is simpler than a phase-shift analysis, and is independent of problems due to inelastic channels (pion production). Of course, the solution does not contain the information of a phase-shift analysis, which gives predictions for all values of $\bar{\theta}$. Nonrelativistic equations relating the observables I_0, P, D, R, A, R', A', C_{nn}, and C_{KP} to the complex coefficients are given in a number of review articles[9]; the relativistically correct expressions are given by Sprung.[10] These observables are calculated in terms of traces of the form $\frac{1}{4}\mathrm{Tr}(M^{+}\boldsymbol{\sigma}^{(1)}\cdot\hat{a}M\boldsymbol{\sigma}^{(1)}\cdot\hat{b})/I_0$, where $\hat{a}$ is the final-state unit vector along which the spin is measured, and $\hat{b}$ is the initial-state unit vector along which the spin is prepared. The observables are therefore bilinear in the complex amplitudes, and in order to obtain a unique solution for the nine unknowns more than nine measurements at a single angle and energy should be used. In the experiment reported here, nine independent quantities were measured, but four of them were at the supplementary angle $\pi-\bar{\theta}$. [Actually 10 quantities were measured, but if T invariance is assumed, they are not all independent. The independent quantities may be chosen as $P(65°)$, $D(65°)$, $R(65°)$, $A(65°)$, $R'(65°)$, $D(115°)$, $R(115°)$, $A(115°)$, and $R'(115°)$.] However, the complex coefficients have simple transformation properties under $\bar{\theta}\to\pi-\bar{\theta}$, so that all nine numbers could be used to calculate a, c, m, g, and h at $\bar{\theta}=65°$. Thus,

$$\begin{aligned} a(\bar{\theta})-m(\bar{\theta})&=-2g(\pi-\bar{\theta}),\\ a(\bar{\theta})+m(\bar{\theta})&=-a(\pi-\bar{\theta})-m(\pi-\bar{\theta}),\\ c(\bar{\theta})&=c(\pi-\bar{\theta}),\\ h(\bar{\theta})&=h(\pi-\bar{\theta}). \end{aligned} \quad (10)$$

The number of pieces of experimental data was increased to eleven by adding the correlation coefficient $C_{nn}=0.486\pm0.049$ of Beretvas *et al.*[11] and the differential cross section $I_0=3.62\pm0.15$ mb/sr of Sutton *et al.*[12]

A unique solution to eleven equations which were bilinear in nine unknowns was obtained in the statistical sense, that is, in the sense of good χ^2. A computer program expanded the equations about a set of initial guesses to the parameters, and then minimized

$$\chi^2=\sum_i\frac{[A_i-f_i(\alpha_j)]^2}{\sigma_i^2} \quad (11)$$

with respect to the α_j's. In this equation $A_i\pm\sigma_i$ is the ith experimental datum and $f_i(\alpha_j)$ is the known function of the unknown parameters α_j. The minimization procedure yielded a better set of α's, which were used for the second iteration. A final value $\chi^2=0.5$ was obtained, where $\chi^2=2$ was expected. This solution is listed in Table VI. No other solutions were found. Also listed in Table VI is a set of complex amplitudes calculated from a set of phase shifts supplied by MacGregor.[13] The input data for the phase-shift fit included the data presented in this experiment, as well as data at neigh-

[8] C. R. Schumacher and H. A. Bethe, Phys. Rev. **121**, 1534 (1961).

[9] See, for example, H. P. Stapp, Ann. Rev. Nucl. Sci. **10**, 292 (1960).

[10] D. W. L. Sprung, Phys. Rev. **121**, 925 (1961).

[11] A. Beretvas, N. E. Booth, C. Dolnick, R. J. Esterling, R. E. Hill, J. Scheid, D. Sherden, and A. Yokosawa, Rev. Mod. Phys. **39**, 536 (1967).

[12] R. B. Sutton, T. H. Fields, J. G. Fox, J. A. Kane, W. E. Mott, and R. A. Stallwood, Phys. Rev. **97**, 783 (1955).

[13] M. H. MacGregor, R. A. Arndt, and R. M. Wright, Phys. Rev. **169**, 1128 (1968); M. H. MacGregor (private communication).

TABLE VI. Results of the solution for the M-matrix elements. The over-all phase was specified by matching the phase of the coefficient "c" to the phase obtained from the phase-shift solution of MacGregor *et al.* The phase-shift solution was obtained by using all available data in the neighborhood of 430 MeV, including the results of this experiment. The units are (millibarns)$^{1/2}$.

	Real part	Imaginary part
	This experiment	
a	-0.424 ± 0.085	0.573 ± 0.062
m	0.327 ± 0.085	-0.094 ± 0.062
c	0.229 ± 0.0	1.034 ± 0.022
g	0.390 ± 0.023	0.218 ± 0.048
h	-0.368 ± 0.027	0.167 ± 0.048
	Phase-shift solution	
a	-0.552 ± 0.019	0.473 ± 0.025
m	0.235 ± 0.017	0.025 ± 0.030
c	0.233 ± 0.036	1.043 ± 0.027
g	0.347 ± 0.013	0.140 ± 0.016
g	-0.414 ± 0.040	0.235 ± 0.054

boring energies and other c.m. angles. The two sets are obviously of the same character, and also have the same form as the original 310-MeV solution No. 1 of MacGregor, Moravcsik, and Stapp.[14] The observables I_0, C_{nn}, P, D, R, A, and R' calculated from these two sets of amplitudes agree with the input data (Table V) within one standard deviation.

A test of parity invariance in p-p scattering is also contained in the data. If parity is conserved, all of the up-down asymmetries δ with the solenoid off in Table I should vanish. The formula for the final polarization with the solenoid off if parity is not conserved can be written from the general formula of Thorndike,[15] and is

$$I_P\langle\boldsymbol{\sigma}_f\rangle = I_0[(P+D\langle\boldsymbol{\sigma}_i\cdot\hat{n}_i\rangle)\hat{n}_f+(P_s+\Delta\langle\boldsymbol{\sigma}_i\cdot\hat{n}_i\rangle)\hat{s}_f + (P_{k'}+\Delta'\langle\boldsymbol{\sigma}_i\cdot\hat{n}_i\rangle)\hat{k}_f]. \quad (12)$$

The $\hat{n}_f$ term is identical to the $\hat{n}_f$ term in Eq. (1). The four quantities in the $\hat{s}_f$ and $\hat{k}_f$ terms represent possible final polarization components in the scattering plane due to parity violation in the p-p interaction. In writing Eq. (12) it has been assumed that $\boldsymbol{\sigma}_i$ was parallel to $\hat{n}_i$ when the solenoid was off. For this to be true, parity must be conserved in the initial p-beryllium scattering inside the cyclotron, and the spin must not precess out of the vertical direction in leaving the cyclotron fringing field. These assumptions, while plausible, were not independently tested. The terms P_s and $P_{k'}$ also could appear in the up-down asymmetries with the solenoid on, and they should not reverse with the solenoid. The hypothesis that $\delta_+ = -\delta_-$ in the absence of instrumental bias depends on parity conservation. To obtain a consistent fit to the quantities P_s, $P_{k'}$, Δ, and Δ', the four solenoid-off asymmetries δ_A, δ_B, δ_C, δ_D were used in conjunction with the average asymmetries $\frac{1}{2}(\delta_+ + \delta_-)$, for each geometry $ABCD$. Thus there were eight experimental quantities. The number of unknowns was increased to six by allowing for two biases, a strong B_2 bias (geometries B and D) and a weak B_2 bias (geometries A and C). A good χ^2 was obtained with a strong bend bias $b_1 = +0.0107\pm0.0017$, a weak bend bias $b_2 = -0.0017\pm0.0023$, and the following parity-violating terms:

$$\begin{aligned} P_s &= -0.0062\pm0.0036, \\ P_{k'} &= +0.0095\pm0.0029, \\ \Delta &= -0.031\ \pm0.015, \\ \Delta' &= -0.025\ \pm0.018. \end{aligned} \quad (13)$$

The statistical errors on P_s and $P_{k'}$ were very small because there was a very large amount of data with the solenoid on. $P_{k'}$ is over three standard deviations from zero, but this is believed due to the presence of nonstatistical errors in the hypotheses made above to solve this particular problem, rather than a parity-violating effect.

The main conclusion to be drawn from this experiment is that the p-p scattering phase-shift analysis, in the form in which it has existed for several years, can be considered unique. Precision measurements of the triple-scattering parameters at other angles in the 400-MeV energy region may serve to determine certain phase shifts to greater accuracy, but they will not change the basic form of the solution. The phase-shift analysis can be used with confidence to predict values for the observables. Indeed, as emphasized in Ref. 13, p-p scattering can be well described by a phase-shift analysis between 0 and 450 MeV.

ACKNOWLEDGMENTS

We wish to thank H. Hinterberger and the staff of the Chicago synchrocyclotron for efficient machine operation during a lengthy experiment. J. Barney constructed much of the electronic equipment. We are indebted to Dr. M. H. MacGregor for many helpful communications.

[14] M. H. MacGregor, M. J. Moravcsik, and H. P. Stapp, Phys. Rev. 116, 1248 (1959).
[15] E. H. Thorndike, Phys. Rev. 138, B586 (1965).